Sparse Channel Estimation for IRS-Aided Systems Exploiting 2-D Sparse Arrays

Mirza Asif Haider, Md. Waqeeb T. S. Chowdhury, and Yimin D. Zhang

Department of Electrical and Computer Engineering, Temple University, Philadelphia, PA 19122, USA

Abstract—Intelligent reflecting surface (IRS) is a promising next-generation technology for increasing channel capacity and reducing power consumption. In this paper, we present a novel IRS configuration consisting of a small number of active elements in an optimized L-shaped sparse array to separately estimate the channels between the base station and the IRS, and the channel between multiple user equipment and the IRS. Structured matrix completion techniques are used to attain superior direction-of-arrival estimation performance with an increased number of degrees of freedom. The training overhead is minimized in the proposed system and is not directly related to the number of IRS reflecting elements. The proposed sparse array strategy simultaneously resolves multiple sources with a high accuracy and outperforms the L-shaped uniform array counterpart using the same number of active elements. The effectiveness of the proposed strategy is confirmed using simulation results.

Keywords: Intelligent reflecting surface, active elements, sparse array, structured matrix completion, channel estimation.

I. INTRODUCTION

Intelligent reflecting surface (IRS) has the capability of reconfiguring the wireless channel between the communicating nodes and is considered as a promising next-generation technology for 5G and beyond [1]. An IRS consists of a large planar surface with passive elements that can control the phase of the incident signals and thereby transmit the reflected signals in the desired directions. As such, IRS creates an extra link between the base station (BS) and user equipment (UE) by exploiting a low-cost large-size fully passive two-dimensional (2-D) array [2].

Achieving the full potential of IRS requires estimation of the complete channel state information (CSI). Compared to signals in the sub-6 GHz band, millimeter wave (mmWave) signals are naturally less scattering and thus sparse. By taking advantage of such channel sparsity, efficient compressive sensing techniques can be applied to perform sparse channel estimation [3–5]. In [5], multi-user joint channel estimation was formulated as a multi-user joint sparse matrix recovery problem based on the common channel between the BS and the IRS. However, because the sparsity in the angular cascaded channel is less significant, its CSI estimation is less effective compared to that in conventional communications [6]. In [4], the double structured sparsity of the angular cascaded channel involving the common non-zero rows and the partially common non-zero columns of the received sparse signal was solved by using the double-structured orthogonal matching pursuit (DS-OMP) algorithm. However, the assumption that common channels

are shared not only between the BS and the IRS but also between the UE and the IRS may not be practically feasible for mobile users. For multi-antenna users, another way to estimate the channel parameters of the BS-IRS-UE sparse channels is through the use of atomic norm minimization. In all channel estimation techniques discussed above, All IRS elements are passive and the number of pilot overhead depends on the number of these passive elements [7–11].

An attractive alternative effective solution is to use a hybrid analog/digital architecture [12]. By utilizing a small number of active elements, an IRS can further aid in high-precision performance in terms of channel estimation and channel reconfiguration. Because equipping each IRS element with a separate radio frequency (RF) front-end circuit requires high hardware and computational complexities [13], only a small number of IRS elements are made active to keep a low complexity. Toward this end, random deployment of a small number of active IRS elements is proposed in [3]. In [14], an L-shaped array of uniformly placed active elements was considered and channel estimation was performed by estimating the direction-of-arrival (DOA) and the associate gain of each path.

In this paper, we develop a new approach to perform channel estimation using sparse active elements in a rectangular IRS. The proposed approach enables separate estimation of the BS-IRS channel and the UE-IRS channel with a reduced number of pilot overhead. Because the BS and IRS are typically placed in fixed positions, the BS-IRS channel can be considered stable over a long time. On the other hand, the UEs are cellular devices and their channel may vary rapidly, thereby necessitating frequent channel estimation between the UEs and the IRS. The two linear arrays that constitute the L-shaped array have their active elements placed in a sparse manner, and the optimized non-redundant array with minimum array aperture (ONRA) structure developed in [15] is used as an example. Separate sparse covariance matrices are formulated based on the two constituting linear arrays of the IRS, and the matrix interpolation technique is employed to fully interpolate Hermitian-Toeplitz covariance matrices. The multiple signal classification (MUSIC) algorithm is used to separately estimate the azimuth and elevation DOAs which are then paired. At last, the path gains are calculated to produce the full geometric BS-IRS-UE CSI corresponding to each UE. Simulation results verify that the proposed L-shaped sparse
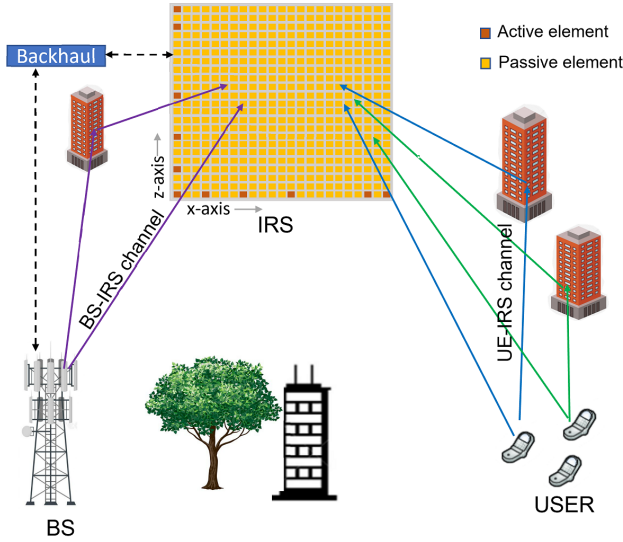
Fig. 1: The BS-IRS-UE channel model.

Fig. 2: The transmission frame structure.

structure outperforms the L-shaped array using uniform linear structure given the same number of the active elements [14].

Notations: We use lower-case (upper-case) bold characters to denote vectors (matrices). In particular, $\mathbf{I}_N$ denotes the $N \times N$ identity matrix. $(.)^{\mathrm{T}}$ and $(.)^{\mathrm{H}}$ respectively represent the transpose and conjugate transpose of a matrix or a vector, and $(\cdot)^{\dagger}$ represents Moore-Penrose inverse of a matrix. In addition, $\|\cdot\|_{\mathrm{F}}$ denote the Frobenius norm, $\otimes$ is the Kronecker product, $\odot$ is the Hadamard product, $\mathcal{T}(\boldsymbol{x})$ denotes the Hermitian and Toeplitz matrix with $\boldsymbol{x}$ as its first column, and $\mathrm{Tr}(\cdot)$ represents the trace operator. Furthermore, $[\mathbf{A}]_{u,v}$ denotes the (u,v)-th element of matrix $\mathbf{A}$, $[\mathbf{A}]_{:,v}$ denotes the v-th column of matrix $\mathbf{A}$, and $\mathbf{A} \succeq$ denotes matrix $\mathbf{A}$ to be positive semidefinite. $\mathbb{E}[\cdot]$ is the statistical expectation operator.

II. SYSTEM MODEL

Consider an IRS-enhanced multiple-input multiple-output (MIMO) downlink communication system that consists of a planar IRS with N reflecting elements, a BS with vertically placed M_T-antenna linear array, and K single-antenna users, as shown in Fig. 1. Among the N reflecting elements, $\bar{N}$ elements are active and are arranged in a sparse L-shaped structure. Assuming a narrowband signal model, the downlink channel matrix between the BS and the IRS can be expressed as:

$$\mathbf{H}_{\mathrm{BS,IRS}} = \sum_{l=1}^{L} \alpha_l \mathbf{a}_{\mathrm{IRS}}(\theta_l^{\mathrm{IRS}}, \phi_l^{\mathrm{IRS}}) \mathbf{a}_{\mathrm{BS}}^{\mathrm{H}}(\theta_l^{\mathrm{BS}}), \quad (1)$$

where L denotes the number of paths between the BS to the IRS, α_l is the path gain of the l-th path, $\theta^{\mathrm{BS}} \in [0, \pi/2]$ is the effective elevation direction-of-departure (DOD) from the BS with respect to the z axis, whereas $\theta_l^{\mathrm{IRS}} \in [0, \pi/2]$ and $\phi_l^{\mathrm{IRS}} \in [-\pi/2, \pi/2]$ are respectively the elevation and azimuth angles for the IRS during BS-IRS channel estimation.
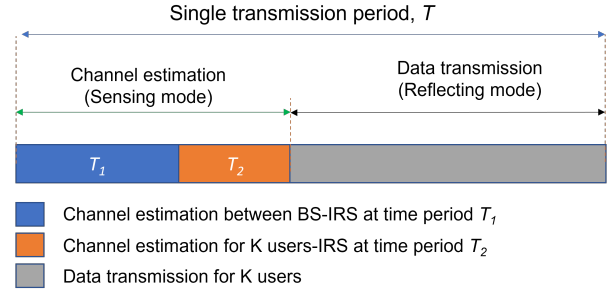
Assuming half-wavelength spacing between BS antennas, the steering vector $\mathbf{a}_{\mathrm{BS}}(\theta)$ of the M_T-element array at the BS is expressed as:

$$\mathbf{a}_{\mathrm{BS}}(\theta) = [1, e^{-j\frac{2\pi}{\lambda}d\sin(\theta)}, \ldots, e^{-j\frac{2\pi}{\lambda}d(M_T-1)\sin(\theta)}]^{\mathrm{T}}, \quad (2)$$

where λ is the wavelength and $d = \lambda/2$. For an N-element IRS uniform rectangular array separated by d, the 2-D steering vector $\mathbf{a}_{\mathrm{IRS}}(\phi, \theta)$ can be written as [16]:

$$\mathbf{a}_{\mathrm{IRS}}(\phi, \theta) = \mathbf{a}_z(\phi) \otimes \mathbf{a}_x(\theta), \quad (3)$$

where

$$\mathbf{a}_x(\phi) = [1, e^{-j\frac{2\pi}{\lambda}d\sin(\phi)}, \ldots, e^{-j\frac{2\pi}{\lambda}d(N_x-1)\sin(\phi)}]^{\mathrm{T}}, \quad (4)$$

$$\mathbf{a}_z(\theta) = [1, e^{-j\frac{2\pi}{\lambda}d\sin(\theta)}, \ldots, e^{-j\frac{2\pi}{\lambda}d(N_z-1)\sin(\theta)}]^{\mathrm{T}}, \quad (5)$$

and N_x and N_z respectively denote the number of elements in the x-axis and z-axis on the IRS surface.

On the other hand, since each UE contains a single antenna, the channel between the IRS and user k is denoted as

$$\mathbf{h}_{\mathrm{IRS},U_k} = \sum_{l_k=1}^{L_k} \beta_{l_k} \mathbf{a}_{\mathrm{IRS}}^{\mathrm{H}}(\theta_{l_k}^{\mathrm{IRS}}, \phi_{l_k}^{\mathrm{IRS}}), \quad (6)$$

where L_k denotes the number of paths between user k and the IRS, β_{l_k} is the path gain of the l_k-th path, $\theta_{l_k}^{\mathrm{IRS}} \in [0, \pi/2]$ and $\phi_{l_k}^{\mathrm{IRS}} \in [-\pi/2, \pi/2]$ are respectively the elevation and azimuth angles of the l_k-th UE-IRS channel from the IRS. Because the direct paths between the BS and the UEs are considered obstructed, the corresponding direct channel is not formulated.

We assume that the channel is constant during a transmission interval T, as shown in Fig. 2. During the time interval T_1, the transmit antennas sequentially transmit their respective pilot signals to estimate the channels between the BS and the IRS [17]. The m-th transmit antenna uses a time period of $\dot{T}_m$ to transit its pilot signal such that $\sum_m^{M_T} \dot{T}_m = T_1$. We assume that the time interval T_1 is equally distributed to all M_T transmit antennas, i.e., $\dot{T}_m = T_1/M_T$ for $m = 1, ..., M_T$.

During the time interval T_2, the channels between the IRS and the K users are estimated. It is noted that, during the channel estimation period, the active elements in the IRS work in a sensing mode. On the other hand, during the data transmission period, all the active and passive elements of the IRS work as passive reflectors.

The DOAs and channel gains estimated at the IRS for both the uplink and downlink channels are sent to the BS via a two-way backhaul link, allowing the BS to estimate the overall BS-IRS-UE channel.

III. 2-D DOA AND PATH GAIN ESTIMATION

As previously stated in Section I, using a small number of active elements in the IRS improves the channel estimation performance while reducing the computational complexity. Configuring the active sensor locations in a rectangular array is much more complicated compared to sparse linear arrays. In this paper, we design a sparse array configuration that ensures minimal mutual coupling among the active elements, and matrix interpolation techniques are utilized to generate virtual lags and improve the channel estimation performance.

A. Received Signals at IRS for BS-IRS Channel Estimation

During the sensing mode, the IRS receives signals from the BS through its active elements. It is assumed that far-field signals impinge on the IRS from L paths, and the DOAs corresponding to the L-shaped sparse array are $\{\phi_l, \theta_l\}$ for $l = 1, \cdots, L$.

The output signal vectors at the two IRS subarrays corresponding to the x-axis and the z-axis are respectively given as [16, 18]:

$$\mathbf{x}(t) = \sum_{l=1}^{L} \mathbf{a}_X(\phi_l)\alpha_l \mathbf{a}_{BS}^{H}(\theta_m)\mathbf{s}_l(t) + \mathbf{n}_X(t), \qquad (7)$$

$$\mathbf{z}(t) = \sum_{l=1}^{L} \mathbf{a}_Z(\theta_{l_1})\alpha_l \mathbf{a}_{BS}^{H}(\theta_m)\mathbf{s}_l(t) + \mathbf{n}_Z(t), \qquad (8)$$

where $\mathbf{s}(t) = [s_1(t), s_2(t), \cdots, s_L(t)]^{T}$ denotes the source signal vector, $\alpha = \text{diag}(\alpha_1, \alpha_2, \cdots, \alpha_L)$ represent the channel coefficients for the multipath signals, and $\mathbf{n}_X(t)$ and $\mathbf{n}_Z(t)$ are additive white Gaussian noise (AWGN) vectors respectively observed at the two subarrays.

We consider separately spaced active elements with an ONRA structure, respectively denoted as $\mathbb{X}_1$ and $\mathbb{Z}_1$. The positions of the active elements along both the x and the z axes are $0 = p_0, p_1, \cdots, p_{N_x-1}$ and $0 = q_0, q_1, \cdots, q_{N_z-1}$. Denote $W_x = \max(\mathbb{X}_1) + 1$ and $W_z = \max(\mathbb{Z}_1) + 1$. Let $\mathbf{a}_X(\phi_{l_1}) \in \mathbb{C}^{W_x \times 1}$ and $\mathbf{a}_Z(\theta_{l_1}) \in \mathbb{C}^{W_z \times 1}$ denote the steering vectors corresponding to the received DOAs along the x axis and the z axis, respectively. In time period T_1, the BS transmits from the M_T antennas and $\mathbf{a}_{BS}(\theta_m)$ is the corresponding steering vector. During the UE-IRS channel estimation, the received signal is formulated in the same manner. Assuming that noise is independent from the signals, the covariance matrices of $\mathbf{x}(t)$ and $\mathbf{z}(t)$ can be respectively expressed as:

$$\mathbf{R}_{X_{IRS}} = \mathbf{E}[\mathbf{x}(t)\mathbf{x}^{H}(t)] = \mathbf{A}_X\mathbf{R}_s\mathbf{A}_X^{H} + \sigma_n^2\mathbf{I}_{W_x}, \qquad (9)$$

$$\mathbf{R}_{Z_{IRS}} = \mathbf{E}[\mathbf{z}(t)\mathbf{z}^{H}(t)] = \mathbf{A}_Z\mathbf{R}_s\mathbf{A}_Z^{H} + \sigma_n^2\mathbf{I}_{W_z}, \qquad (10)$$

where $\mathbf{R}_s = \text{diag}(\sigma_1^2, \sigma_2^2, \cdots, \sigma_L^2)$, σ_l^2 represents the power of the l-th path signal, and σ_n^2 denotes the noise power.

B. Covariance Matrix Interpolation and DOA Estimation

Because the active elements are sparsely spaced in both the x-axis and the z-axis, the covariance matrices $\mathbf{R}_{X_{IRS}}$ and $\mathbf{R}_{Z_{IRS}}$ become sparse with missing holes. In the following, we consider the matrix interpolation of $\mathbf{R}_{X_{IRS}}$ to obtain a full covariance matrix, and the same approach is applied to $\mathbf{R}_{Z_{IRS}}$. The steering vectors for the sparse array in both axes are represented as:

$$\mathbf{a}_X(\phi) = [1, e^{-j\frac{2\pi p_1}{\lambda}d\sin(\phi)}, \ldots, e^{-j\frac{2\pi(p_{N_x-1})}{\lambda}d\sin(\phi)}]^{T}, \quad (11)$$

$$\mathbf{a}_Z(\theta) = [1, e^{-j\frac{2\pi q_1}{\lambda}d\sin(\theta)}, \ldots, e^{-j\frac{2\pi(q_{N_z-1})}{\lambda}d\sin(\theta)}]^{T}. \quad (12)$$

The matrix interpolation problem along the x-axis is expressed as the following nuclear norm minimization problem [19–21]:

$$\min_{\boldsymbol{w}} \quad \|\mathcal{T}(\boldsymbol{w})\mathbf{V} - \hat{\mathbf{R}}_{X_{IRS}}\|_F^2 + \zeta\text{Tr}\left(\sqrt{\mathcal{T}^{H}(\boldsymbol{w})\mathcal{T}(\boldsymbol{w})}\right),$$
$$\text{s. t.} \quad \mathcal{T}(\boldsymbol{w}) \succeq 0, \tag{13}$$

where $\|\mathcal{T}(\boldsymbol{w})\|_* = \text{Tr}(\sqrt{\mathcal{T}^{H}(\boldsymbol{w})\mathcal{T}(\boldsymbol{w})})$ is the nuclear norm of $\mathcal{T}(\boldsymbol{w})$, ζ is a tunable regularization parameter. $\mathbf{V} = \mathbf{v}_p\mathbf{v}_p^{T}$ is the binary mask of the sparse covariance matrix where the g-th element of $\mathbf{v}_p$, $g \in \{p_0, p_1, \cdots, p_{N_x-1}\}$, is given as

$$\langle\mathbf{v}_p\rangle_g = \begin{cases} 1, & gd \in \mathbb{X}_1, \\ 0, & \text{otherwise.} \end{cases} \tag{14}$$

Denote the interpolated covariance matrices as $\hat{\mathbf{R}}_X \in \mathbb{C}^{W_x \times W_x}$ and $\hat{\mathbf{R}}_Z \in \mathbb{C}^{W_z \times W_z}$ for the x- and the z-axes, respectively. The computational complexities required to recover $\hat{\mathbf{R}}_X$ and $\hat{\mathbf{R}}_Z$ are $\mathcal{O}(W_x^2)$ and $\mathcal{O}(W_z^2)$, respectively [22]. As both interpolated covariance matrices contain all elements defined in full uniform arrays, subspace-based methods, such as MUSIC, can be applied to $\hat{\mathbf{R}}_X$ to estimate the azimuth and elevation DOAs at the IRS for the BS-IRS multipath signals.

C. Pair-Matching for 2-D DOA Estimation

When there are multiple incident signals at the IRS, different combinations between the azimuth and elevation angles become possible. Therefore, it is important to determine the pairing between the estimated azimuth and elevation angles. The array manifold matrix can be constructed based on the estimated azimuth angles as

$$\hat{\mathbf{A}}_X = [\mathbf{a}_X(\hat{\phi}_1), \mathbf{a}_X(\hat{\phi}_2), \cdots, \mathbf{a}_X(\hat{\phi}_L)]. \tag{15}$$

The cross-covariance matrix between $\mathbf{x}(t)$ and $\mathbf{z}(t)$ is computed as

$$\mathbf{R}_{XZ} = \mathbf{E}[\mathbf{x}(t)\mathbf{z}^{H}(t)] = \mathbf{A}_X\mathbf{R}_S\mathbf{A}_Z^{H}. \tag{16}$$

The steering matrix $\hat{\mathbf{A}}_Z$ can be obtained as [16]

$$\hat{\mathbf{A}}_Z = (\mathbf{R}_S^{-1}\hat{\mathbf{A}}_X^{\dagger}\mathbf{R}_{XZ})^{H}, \tag{17}$$

where $\hat{\mathbf{A}}_Z = [\mathbf{a}_z(\hat{\theta}_1), \mathbf{a}_z(\hat{\theta}_2), \cdots, \mathbf{a}_z(\hat{\theta}_L)] \in \mathbb{C}^{W_z \times L}$. Therefore, for the l-th path with $l = 1, 2, \cdots, L$, we can reconstruct the covariance matrix as

$$\hat{\mathbf{R}}_{Z_l} = [\hat{\mathbf{A}}_Z]_{:,l}[\mathbf{R}_S]_{l,l}[\hat{\mathbf{A}}_Z]_{:,l}^{H}. \tag{18}$$

Using this result, the elevation angle is estimated using the MUSIC algorithm as

$$\hat{\theta}_l = \arg\max_{\boldsymbol{\theta}} \frac{1}{\mathbf{a}_Z^H(\theta)\mathbf{G}_l\mathbf{G}_l^H\mathbf{a}_Z(\theta)}, \quad (19)$$

where $\mathbf{G}_l$ is the noise subspace of matrix $\hat{\mathbf{R}}_{Z_l}$. From the paired azimuth and elevation angle estimates we can generate the steering matrix of the IRS for the BS-IRS channel as $\hat{\mathbf{A}}_{\text{IRS}} = \left[\hat{\mathbf{a}}_{\text{IRS}}(\phi_1^{\text{IRS}}, \theta_1^{\text{IRS}}), \cdots, \hat{\mathbf{a}}_{\text{IRS}}(\phi_L^{\text{IRS}}, \theta_L^{\text{IRS}})\right] \in \mathbb{C}^{W_x \times W_z}$.

D. Path Gain Estimation

To estimate the path gain of the BS-IRS channel, the BS antennas transmit pilot signals sequentially. For example, the first antenna transmits pilot signal $\mathbf{S} = [\mathbf{s}(1), \mathbf{s}(2), \cdots, \mathbf{s}(\dot{T}_1)] \in \mathbb{C}^{L \times \dot{T}_1}$. Note in this subsection that we omit the antenna index in the notations for simplicity. At the IRS, the received signal at the z-direction subarray is,

$$\mathbf{Y}_Z = \mathbf{A}_Z \mathbf{B} \mathbf{A}_{\text{BS}}^H \mathbf{S} + \mathbf{N}_Z, \quad (20)$$

where $\mathbf{B} = \text{diag}(\alpha_1, \alpha_2, \cdots, \alpha_L)$ is the path gain matrix, $\hat{\mathbf{A}}_{\text{BS}} = [\mathbf{a}_{\text{BS}}(\hat{\theta}_1), \mathbf{a}_{\text{BS}}(\hat{\theta}_2), \cdots, \mathbf{a}_{\text{BS}}(\hat{\theta}_L)] \in \mathbb{C}^{M_T \times L}$ is the array manifold of the IRS along the z axis and BS, and $\mathbf{N}_Z \sim \mathcal{CN}(0, \sigma_n^2 \mathbf{I}_{pN_z-1})$. As the path gains are identical for the x- and z-direction subarrays, computation in one direction will suffice. The path gain matrix $\mathbf{B}$, denoted as $\hat{\mathbf{B}} = \text{diag}(\hat{\alpha}_1, \hat{\alpha}_2, \cdots, \hat{\alpha}_L)$, can be estimated as

$$\hat{\mathbf{B}} = \boldsymbol{\Omega}^\dagger \mathbf{Y}_Z \mathbf{S}^\dagger, \quad (21)$$

where $\boldsymbol{\Omega} = [\mathbf{a}_Z(\hat{\theta}_1) \odot \mathbf{v}_q, \cdots, \mathbf{a}_Z(\hat{\theta}_L) \odot \mathbf{v}_q]\mathbf{A}_{BS}^H$, where $\mathbf{v}_q$ is defined along the z-axis in the same way as $\mathbf{v}_p$ defined in (14).

IV. SIMULATION RESULTS

In this section, we provide simulation results to demonstrate the effectiveness of the proposed channel estimation scheme. We consider a BS with $M_T = 2$ transmit antennas, an IRS with $N = W_x \times W_z = 529$ reflecting elements, and $K = 2$ single-antenna users. Out of the 529 IRS reflecting elements, $\bar{N} = 11$ elements are active. The x- and z-direction linear subarrays in the L-shape sparse active array each consists of 6 sensors, and the 0-th reference sensor is shared by both subarrays. Following the ONRA configuration, the positions of the active elements along the x- and the z-axes are $\mathbb{X}_1 = \mathbb{Z}_1 = \{0, 3, 7, 12, 20, 22\}\lambda/2$. The corresponding nonnegative lags are computed as $\mathbb{D}_{\text{self}}^{X_1} = \mathbb{D}_{\text{self}}^{Z_1} = \{0, 2, 3, 4, 5, 7, 8, 9, 10, 12, 13, 15, 17, 19, 20, 22\}\lambda/2$.

We assume $L = 2$ paths with path gains of (0.2, 0.25) for the BS-IRS channel and $L_k = 2$ paths from IRS to each of the two users with respective path gains (0.2, 0.4) and (0.6, 0.85). The input signal-to-noise ratio (SNR) is assumed to be 5 dB. The root mean-square error (RMSE) between the true channels and the estimated channels is plotted in Fig. 3 with respect to the number of snapshots, where solid curves represent the RMSE obtained by using the ONRA sparse structure whereas dashed curves represent the RMSE obtained when the active elements
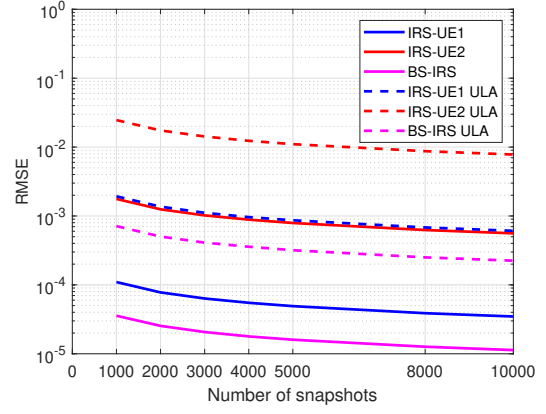

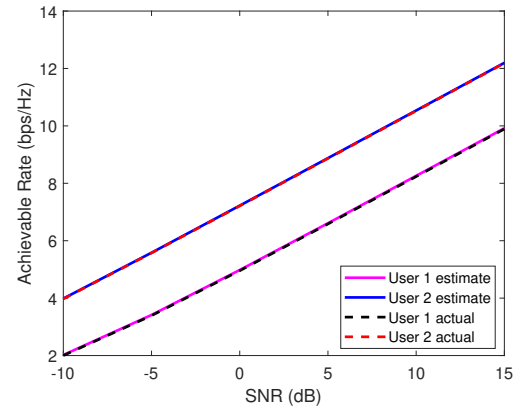Fig. 3: RMSE versus number of snapshots (input SNR = 5 dB).

Fig. 4: Achievable bit-rate versus input SNR ($T_1 = T_2 = 1,000$ snapshots).

are uniformly placed. Results clearly show that the IRS with L-shaped ONRA active elements achieves significantly higher channel estimation accuracy than that using uniform linear subarrays with the same number of $\bar{N} = 11$ active elements.

Fig. 4 shows the achievable bit-rate with respect to the input SNR, where $T_1 = T_2 = 1,000$ data snapshots are assumed. The results confirm that the available bit rates for both users corresponding to the true and estimated channels well coincide, thus demonstrating the accuracy of the channel estimation in terms of the achievable bit-rate from Shannon's channel capacity theorem.

V. CONCLUSION

In this paper, we have shown that employing active elements in the IRS in a sparse manner outperforms the counterpart that employs active elements exploiting uniform linear subarrays. Structured matrix completion and pair-matching algorithms are used to achieve increased array aperture and reduced computational complexity. The effectiveness and precision of the proposed approach have been demonstrated using simulation results.

VI. REFERENCES

[1] W. Long, R. Chen, M. Moretti, W. Zhang, and J. Li, "A promising technology for 6G wireless networks: Intelligent reflecting surface," *J. Commun. and Inform. Networks*, vol. 6, no. 1, pp. 1–16, 2021.

[2] Q. Wu, S. Zhang, B. Zheng, C. You, and R. Zhang, "Intelligent reflecting surface aided wireless communications: A tutorial," *IEEE Trans. Commun.*, vol. 69, no. 5, pp. 3313–3351, May 2021.

[3] A. Taha, M. Alrabeiah, and A. Alkhateeb, "Enabling large intelligent surfaces with compressive sensing and deep learning," *IEEE Access*, vol. 9, pp. 44 304–44 321, 2021.

[4] X. Wei, D. Shen, and L. Dai, "Channel estimation for RIS assisted wireless communications—part II: An improved solution based on double-structured sparsity," *IEEE Commun. Lett.*, vol. 25, no. 5, pp. 1403–1407, 2021.

[5] J. Chen, Y.-C. Liang, H. V. Cheng, and W. Yu, "Channel estimation for reconfigurable intelligent surface aided multi-user MIMO systems," *arXiv preprint arXiv:1912.03619*, 2019.

[6] X. Wei, D. Shen, and L. Dai, "Channel estimation for RIS assisted wireless communications—part I: Fundamentals, solutions, and future opportunities," *IEEE Commun. Lett.*, vol. 25, no. 5, pp. 1398–1402, 2021.

[7] C. Huang, A. Zappone, G. C. Alexandropoulos, M. Debbah, and C. Yuen, "Reconfigurable intelligent surfaces for energy efficiency in wireless communication," *IEEE Trans. Wireless Commun.*, vol. 18, no. 8, pp. 4157–4170, 2019.

[8] Z. Wang, L. Liu, and S. Cui, "Channel estimation for intelligent reflecting surface assisted multiuser communications," in *Proc. 2020 IEEE Wireless Commun. and Networking Conf. (WCNC)*. IEEE, 2020, pp. 1–6.

[9] C. Hu, L. Dai, S. Han, and X. Wang, "Two-timescale channel estimation for reconfigurable intelligent surface aided wireless communications," *IEEE Trans. Commun.*, 2021.

[10] X. Guan, Q. Wu, and R. Zhang, "Anchor-assisted intelligent reflecting surface channel estimation for multiuser communications," in *Proc. 2020 IEEE Global Commun. Conf. (GLOBECOM)*, pp. 1–6.

[11] Z. Wang, L. Liu, and S. Cui, "Channel estimation for intelligent reflecting surface assisted multiuser commu-

nications: Framework, algorithms, and analysis," *IEEE Trans. Wireless Commun.*, vol. 19, no. 10, pp. 6607–6620, 2020.

[12] J. Qiao and M.-S. Alouini, "Secure transmission for intelligent reflecting surface-assisted mmwave and terahertz systems," *IEEE Wireless Commun. Lett.*, vol. 9, no. 10, pp. 1743–1747, 2020.

[13] A. Alkhateeb, O. El Ayach, G. Leus, and R. W. Heath, "Channel estimation and hybrid precoding for millimeter wave cellular systems," *IEEE Sel. Top. Signal Process.*, vol. 8, no. 5, pp. 831–846, 2014.

[14] X. Chen, J. Shi, Z. Yang, and L. Wu, "Low-complexity channel estimation for intelligent reflecting surface-enhanced massive MIMO," *IEEE Wireless Commun. Lett.*, vol. 10, no. 5, pp. 996–1000, 2021.

[15] A. Ahmed and Y. D. Zhang, "Generalized non-redundant sparse array designs," *IEEE Trans. Signal Process.*, vol. 69, pp. 4580–4594, 2021.

[16] F. Wu, F. Cao, X. Ni, C. Chen, Y. Zhang, and J. Xu, "L-shaped sparse array structure for 2-D DOA estimation," *IEEE Access*, vol. 8, pp. 140 030–140 037, 2020.

[17] L. Zheng and D. N. C. Tse, "Diversity and multiplexing: A fundamental tradeoff in multiple-antenna channels," *IEEE Trans. Info. Theory*, vol. 49, no. 5, pp. 1073–1096, 2003.

[18] X. Hu, R. Zhang, and C. Zhong, "Semi-passive elements assisted channel estimation for intelligent reflecting surface-aided communications," *IEEE Trans. Wireless Commun.*, 2021.

[19] C. Zhou, Y. Gu, Z. Shi, and Y. D. Zhang, "Off-grid direction-of-arrival estimation using coprime array interpolation," *IEEE Signal Process. Lett.*, vol. 25, no. 11, pp. 1710–1714, 2018.

[20] S. Zhang, A. Ahmed, Y. D. Zhang, and S. Sun, "DOA estimation exploiting interpolated multi-frequency sparse array," in *Proc. IEEE Sens. Array Multichannel Signal Process. Workshop*, Hangzhou, China, June 2020.

[21] M. W. T. S. Chowdhury and Y. D. Zhang, "Direction-of-arrival estimation exploiting distributed sparse arrays," in *Proc. Asilomar Conf. Signals, Systems, and Computers*, Pacific Grove, CA, Oct. 2021.

[22] Z. Mao, S. Liu, Y. D. Zhang, L. Han, and Y. Huang, "Joint DoA-range estimation using space-frequency virtual difference coarray," *IEEE Trans. Signal Process.*, in press.